Speeding up master slave optical coherence tomography by matrix manipulation

Adrian Podoleanu, Adrian Bradu, Manuel Marques, Sylvain Rivet

Adrian Podoleanu, Adrian Bradu, Manuel Marques, Sylvain Rivet, "Speeding up master slave optical coherence tomography by matrix manipulation," Proc. SPIE 10889, High-Speed Biomedical Imaging and Spectroscopy IV, 1088908 (4 March 2019); doi: 10.1117/12.2511404

SPIE.

Event: SPIE BiOS, 2019, San Francisco, California, United States

Speeding up master slave optical coherence tomography by matrix manipulation

Adrian Podoleanu*[a], Adrian Bradu[a], Manuel Marques[a] and Sylvain Rivet[b]

[a]Applied Optics Group, School of Physical Sciences, University of Kent, Canterbury CT2 7NH, UK
[b]Université de Bretagne Occidentale, IBSAM, Laboratoire OPTIMAG, 6 avenue Le Gorgeu, C.S. 93837, 29238 Brest Cedex 3, France

ABSTRACT

This paper presents the last leg of the evolution of the Master Slave (MS) optical coherence tomography (OCT) technology, towards complex master slave (CMS), where phase information is also delivered. We will show how matrix manipulation of signals can lead to real time display. We have demonstrated that this can be executed on central processing units (CPU)s with no need for graphic processing units (GPU)s, yielding simultaneous display of multiple *en-face* OCT images (C-scans), two cross-section OCT images (B-scans) and an aggregated image, equivalent to a scanning laser ophthalmoscopy (SLO) image when imaging the retina, which is similar to a confocal microscopy image. The same protocol can obviously be applied employing GPUs when using faster acquisition engines, such as multi MHz swept optical sources.

Keywords: master slave, optical coherence tomography, matrix multiplications, real-time operation

1. INTRODUCTION

Both implementations of the Fourier (spectral) domain OCT, spectrometer based (Sp)-OCT and swept source (SS)-OCT, can be used to produce both B-scan and C-scan images with high resolution and high sensitivity. Traditionally, in order to produce a volumetric image, in both implementations, each channeled spectrum acquired while scanning the probing beam over the sample is subject to a fast Fourier transform (FFT). However, before the FFT, several preparatory signal processing steps such as zero padding, spectral shaping, apodization, dispersion compensation or data re-sampling are required to produce high axial resolution and sensitivity images. As all these steps are sequentially executed, the need to perform them impacts the time required to produce images and hampers real-time display.

So far, several techniques involving both hardware and/or software solutions have been demonstrated to successfully correct for the chirp due to non-linearities in the spectrum and dispersion in the interferometer. They either increase the cost or processing time. The accuracy in distance and thickness measurements also depends on how good the chirp correction is.

Master slave (MS) interferometry [1] was introduced to address limitations due to the use of Fourier transforms (FT)s in OCT. Initial proposal of MS protocol was devised around a comparison of two electrical signals. The two signals were proportional to the channeled spectra at the outputs of two interferometers. The optical path difference (OPD) in the master interferometer using two mirrors dictates the depth wherefrom signal is selected by the slave interferometer from the sample (tissue). Its practical implementation then evolved towards replacing the master interferometer with masks (stored templates of channeled spectra acquired for different OPDs). Then, the method was refined by using complex forms of masks, that allow phase processing, method denominated as complex master slave (CMS) interferometry and CMS-OCT [2]. Then further research on speeding the digital implementation of comparison operation, initially performed using 3 FTs, have shown how to employ only two FTs, by storing the FT of the masks [3]. We will present such benchmarks here to illustrate the time requirement by each of the method evaluated. Then further on, we evaluated a method where the multiple comparison operations were replaced by simplified correlations in lag zero. Such correlations can be performed by simple multiplications of channeled spectra, i.e. of each mask from storage (or delivered by the master interferometer) with that from the slave interferometer. This has allowed competing for time with the conventional FT based OCT signal processing but required GPUs [4]. This paper presents the last leg of the evolution of the MS (CMS) technology, where we will show how matrix manipulation of signals can lead to real time display. We have demonstrated that this can be executed on multi-core CPUs with no need to GPUs, for simultaneous display of multiple *en-face* OCT images, of two cross-section images and of an aggregated image.

High-Speed Biomedical Imaging and Spectroscopy IV, edited by Kevin K. Tsia, Keisuke Goda, Proc. of SPIE Vol. 10889, 1088908 · © 2019 SPIE · CCC code: 1605-7422/19/$18 · doi: 10.1117/12.2511404

2. BENCHMARKING OF MASTER SLAVE IMPLEMENTATIONS

Comparison operation using a limited number of multiplications in the calculation of correlation

Initial implementations of the MS method were based on correlation of two channeled spectra followed by a windowing operation. This is equivalent to calculating the comparison result by using a limited number of delays applied to a rectified correlation function:

$$A_p = A(OPD_p) = \sum_{s=-W_p}^{W_p} Comp_{out,s}(p) = \sum_{w=-W_p}^{W_p} \left| \sum_{k=1}^{2E} M_p(k+w) \cdot CS(k) \right|$$

Here *k* is the pixel number along the wavenumber, *k*-coordinate. Such an approach reduces the time required for the comparison operation implemented via correlation. If the windowing filter selects only $W=2W_p+1$ delay points of the correlation result, then this means that out of the total of 4E+1 delays used in the full calculation of correlation, only W delays are retained. Signals of length 2E are multiplied for a reduced number W in Eq. (1).

The experiment performed allowed an evaluation of the time required and resources by the two methods, FFT based OCT conventional method and the novel MS method, both applied to SS-OCT. The results obtained are shown in Tables 1-5. An Intel® Xeon® CPU, model E5646 (clock speed 2.4 GHz, 6 cores) was used. For 200x200 pixels in transversal section, 40,000 channeled spectra are collected in 0.4 s. 1280 spectral points are acquired, i.e. 640 depth points equivalent along the axial coordinate of the A-scans. An FFT operation requires as little as 2.825 µs while correlation takes up to 9.2 µs. If linearization of data is needed, then an A-scan is obtained in 69 microseconds and an *en-face* OCT image only after the cut of the volume (0.22 s), which leads to a time of 3.5 s.

Performing two FFTs (when what is stored at the Master stage are FFTs of the experimental channeled spectra, to implement correlation is obviously longer than a single FFT, but much shorter than the time required for linearization plus FFT. This determines a net advantage of the method presented here for real situations, where the sweeping as well as the spectrometer deliver signals. The one frame volume was acquired in 0.4 s. Then, the production of each *en-face* image using the MSI method takes 368 ms. This leads to a time to produce an *en-face* OCT image using the MSI method of 0.768 s.

To produce 200 cuts, the FFT based conventional method required 47.48 s while the MS method needed 74 s. If GPUs would be used, with parallel processing, such as via a compute unified device architecture (CUDA) platform, NVIDIA, then all 200 calculations can be produced in a single step in parallel during the time required for a single calculation, ~ an estimated 0.62 s for the FFT based method and 0.4 s for the MS method.

When performing the MS method, CUDA can be used to evaluate the comparisons for all points in the A-scan in parallel (correlations). Using P = 640 processors in parallel, an A-scan can be produced using the MS method in the time for a single comparison step (correlation) of 9.2 µs, comparable with the time achieved by the FFT based prior art of 2.825 µs.

All these numerical values demonstrate that the MS based OCT can be implemented in principle with similar acquisition and processing time as the prior art, however with no need for calibration and linearization. In addition, the MS method and MS set-ups allow a quicker production of an *en-face* OCT image.

Table 1: Prior art (FFT based Spectral Domain Interferometry based OCT, using sequential calculations)

Time	Acquisition	FFT	Interpolation	A single *En-face* Cut	200 Cuts	A single *En-face image* (acqusitions +FFT+ Interpolation + 1 cut)	200 *En-face images* (acquisition +FFT+ Interpolation + 200 cuts)
A-scan	10 µs	2.825 µs	69.175 µs	221ms	44.2 s	3.501s	47.48 s
B-scan	2 ms	565 µs	13.835 ms				
Volume	400 ms	113 ms	2.767 s				

Table 2: Master/Slave based OCT, where the comparison consists in correlation evaluated using 3 FFTs

Time	Acquisition	Correlation with one mask	A-scan (1 CS acqusition +640 correlations)	B-scan (200 CS acquisitions +200x640 correlations)	1 *En-face image* (40000 CS acquisitions +correlation)	200 *En-face images* (acqusition +200 correlations)
1 CS	10 µs	9.2 µs	5.881 ms	1.179 s	768 ms	74 s
200 CS	2 ms	1.84 ms				
40,000 CS	400 ms	368 ms				

Table 3: Master/Slave Interferometry based OCT, where the comparison consists in correlation evaluated using 2 FFTs

Time	Acquisition	Correlation with one mask	A-scan (1 CS acqusition +640 correlations)	B-scan (200 CS acquisitions +200x640 correlations)	1 *En-face image* (40000 CS acquisitions +correlation)	200 *En-face images* (acqusition +200 correlations)
1 CS	10 µs	5.25 µs	3.881 ms	0.674 s	610 ms	42.4 s
200 CS	2 ms	1.05 ms				
40,000 CS	400 ms	210 ms				

Table 4: Master/Slave based OCT, where the comparison was performed using cross-correlations using a limited number of multiplications (W = 11).

Time	Acquisition	Correlation with one mask	A-scan (1 CS acquisition +640 correlations)	B-scan (200 CS acquisitions +200x640 correlations)	1 *En-face image* (40000 CS acquisitions +correlation)	200 *En-face images* (acquisition +200 correlations)
1 CS	10 µs	2.3 µs	1.472 ms	0.296 s	493 ms	19 s
200 CS	2 ms	0.46 ms				
40,000 CS	400 ms	93 ms				

Table 5: Correlation with one mask for different number of delay steps W.

W	0	3	11	21	51	101	2001
Time (µs)	0.85	0.95	2.3	4.0	9.0	17.9	34.5

Complex Master Slave based OCT

Numerically, the comparison operation of CMS can be rewritten as a correlation in lag zero, to describe the reflectivity value from a scattering center at an axial position *z,* by:

$$A_z = \sum_{k=1}^{N_k} CS(\varphi_{k,z})\tilde{M}(k,z),$$

Here, $\tilde{M}(k,z)$ are complex-valued, theoretically inferred channeled spectra (complex masks). Using Eq. 2, a B-scan image can be represented in a matrix form as:

$$B_{CMSI} = CS \times \tilde{M}$$

where CS, is a matrix of size $N_x \times N_k$, containing the channeled spectra CS_x, acquired for all lateral pixels $x=1,2,\ldots N_x$ (along a laterally oriented scan), described by:

$$CS = \begin{bmatrix} CS_{11} & CS_{12} & \dots & CS_{1N_x} \\ CS_{21} & CS_{22} & \dots & CS_{2N_x} \\ \vdots & \vdots & \ddots & \vdots \\ CS_{N_k1} & CS_{N_k2} & \dots & CS_{N_kN_x} \end{bmatrix} = \begin{bmatrix} CS_1 & CS_2 & \cdots & CS_{N_x} \end{bmatrix}$$

Each column of this matrix contains the N_k components of the channeled spectrum acquired for each lateral pixel, CS_x. Each of the components CS_{kx} is obtained after digitization. $\tilde{M}(k,z)$ is a matrix of size $N_k \times N_z$, described by:

$$\tilde{M} = \begin{bmatrix} \tilde{M}_{11} & \tilde{M}_{12} & \dots & \tilde{M}_{1N_k} \\ \tilde{M}_{21} & \tilde{M}_{22} & \dots & \tilde{M}_{2N_k} \\ \vdots & \vdots & \ddots & \vdots \\ \tilde{M}_{N_z1} & \tilde{M}_{N_z2} & \dots & \tilde{M}_{N_zN_k} \end{bmatrix} = \begin{bmatrix} \tilde{M}_1 \\ \tilde{M}_2 \\ \vdots \\ \tilde{M}_{N_z} \end{bmatrix}$$

Here, each row of the matrix $\tilde{M}$ is a complex signal of N_k components representing a mask produced for each axial position $z = 1,2,\dots N_z$. The channeled spectra used in Eq. (4) to produce the B-scans, do not require any preparation, while the resulting B-scan images are completely free of eventual unbalanced dispersion or decoding non-linearities.

A CMS based cross-sectional image is generated according to the following procedure:

(i) With a high reflector as object, two or more experimental channeled spectra corresponding to different but equally spaced axial positions are stored. This step is performed only once for a given experimental set-up, before data acquisition.

(ii) The experimental channeled spectra recorded at the step above are then used to theoretically infer N_z complex masks (matrix $\tilde{M}$ as described in [2, 5]. This step, that is performed before data acquisition, needs to be repeated only if the axial range displayed in the B-scan image is to be modified.

(iii) A cross-sectional image is produced by multiplying two matrices. This step is performed as soon as raw data corresponding to a B-scan is acquired.

The size in pixels of the cross-sectional MS-OCT image produced in Eq. (3) is $N_x \times N_z$, different from that described by Eq. (5) for the FT case, which is $N_x \times N_k/2$. This axial range difference triggers a discussion on an important aspect: when using the conventional strategy, FFT based, the axial range of each A-scan scales from $z_{min} = 0$ to a maximum value z_{max}, determined by the sampling speed of the digitizer, hence by the number of sampling points N_k used to digitize the channeled spectrum. A modification of the axial range of interest (ROI), if needed, can only be achieved by effectively cropping the cross-section image, while a modification of the number of sampling points of the ROI is only possible by zero-padding the channeled spectra before FFT. In CMS, the axial length of the axial region of interest ROI is completely independent on the number of digitized points N_k. This opens the possibility of sparse signal processing. In addition, the axial range of interest as well as its coverage is adjustable by selecting the set of complex masks $\tilde{M}$ in terms of their axial position and increment between their depths.

Comparison FFT to CMS operation for different number of spectral points Nk.

Using the same computer as above, a benchmarking was evaluated. Fig. 1 illustrates benchmarking of CMS versus number of spectral points N_k, showing the time taken to evaluate an FFT in $N_{k/2}$ points and a number of depth calculations up to $N_{k/2}$ using CMS. Up to $N_k = 128$, CMS is faster than the FFT in producing $N_{k/2}$ points data than an FFT of $N_{k/2}$ points. For larger N_k values, $N_k = 256$, only 64 points can be delivered by the CMS in a shorter time than the FFT. Similarly, for $N_k = 16{,}384$ points, only 32 points can be delivered by the CMS in a shorter time than the FFT, which delivers A-scans of 8,192 points.

All these calculations have not included any re-sampling or correction in the FFT procedure. They show that the CMS can produce a sufficient number of *en-face* images even when the number of spectral points is large, as necessary for long coherence swept sources [6]. In the example above of $N_k = 16{,}384$ points, C-scan images from 32 depths can be

delivered by the CMS, while the FFT requires first assembly of the volume of data. This is equivalent to a sparse representation in real-time of the volume.

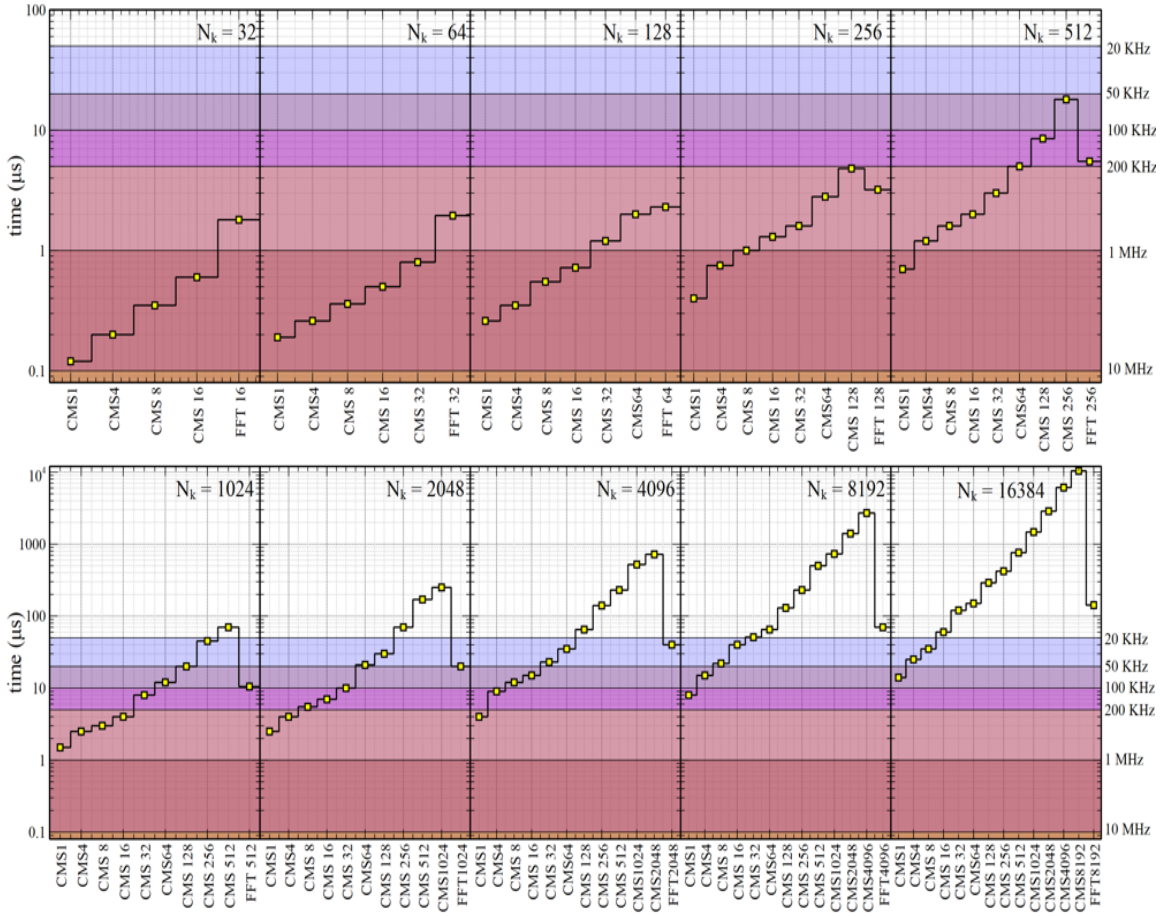

Fig. 1. Benchmarking of CMS/FFT execution time versus number of spectral points N_k, showing the time taken to evaluate an FFT in $N_k/2$ points and the time to evaluate various number of points using CMS. The right vertical axis depicts the equivalent A-line rates for the spectrometer/swept-source based system being used with either method.

In Fig. 1, along the left vertical axis we present the time that a multi-core processor needs to produce several points in the A-scan (1, 2, … $N_k/2$), when different numbers of sampling points are used to digitize the experimental spectra (N_k = *32, 64 …16,384).* When using the FFT method, we will always have $N_{k/2}$ points axially. Along the right vertical axis, we present the sweeping rate of several swept sources (or inverse of reading times of the cameras within the spectrometer in case Sp-OCT method is used, or equivalent A-scan rate). It is quite clear that with the current capabilities of our computer, either method, CMS or FFT cannot produce points along the axial direction in real-time (i.e. the processing time to be faster than the data acquisition time) if a swept source sweeping at 10 MHz is employed. However, at 9 MHz, CMS can provide in real-time one point axially if the spectrum is sampled into 32 points. For this situation, (32 sampling points) FFT can only operate in real time at 450 kHz. At 1MHz, CMS can provide 32 axial points when the spectrum is sampled into 64 points. The FFT approach can be used to deliver real-time A-scans when using 64 sampling points only when the acquisition is performed at less than 550 kHz. In a typical OCT instrument, spectra are sampled into 1024 – 2048 points. If we look at the situation where N_k = 1024, we can notice that CMS and FFT can perform at the same speed when data acquisition is 100 kHz, however, for this particular case, CMS generates 64 points axially only while FFT 512. At 200 kHz, the CMS only can perform data processing in real-time, but only by restricting the number of points that the reflectivity is evaluated to 16 or less. All these comparisons should keep in mind that calculation for the FFT conventional method has not included any correction of chirp.

3. CONCLUSIONS

The use of matrix multiplications to calculate cross-correlations has revolutionized the MS approaches. This has allowed generation of OCT images in real-time, without the need of GPUs or FPGAs. Even when highly optimized, the MS approach based on cross-correlation cannot compete with the CMS in terms of processing time. MS can generate A-scans of $N_k/2$ axial points in around 5.8 ms (Table 2), when 3 FFTs are employed to cross-correlate spectra and in 3.8 ms (Table 3) when only 2 FFTs are employed. This does not allow real-time operation of the instrument, not even in situations where the cross-correlation is restricted to W = 1, in which case an A-scan can be produced in 1.4 ms (Table 4). The CMS, based on matrix multiplication, allows for higher processing speeds. For spectra digitized into $N_k = 1024$ sampling points corresponding to $N_k/2$ points axially, an A-scan can be produced in ~ 50 μs (Fig. 1). This is not only tens of times faster than the cross-correlation implementation but allows CMS to compete even with the FFT when there is no need to compensate for unbalanced dispersion and chirp in reading the spectrum.

ACKNOWLEDGMENTS

The authors wish to acknowledge the following funding sources: H2020 Marie Sklodowska-Curie Actions (MSCA) (625509), Engineering and Physical Sciences Research Council (EPSRC) (`REBOT', EP/N019229/1), H2020 European Research Council (ERC) (`ADASMART', 754695), National Institute for Health Research Biomedical Research Centre at Moorfield Eye Hospital NHS Foundation Trust (NIHR), the UCL Institute of Ophthalmology, University College London, and the Royal Society Wolfson research merit award.

REFERENCES

[1] Podoleanu, A. and Bradu, A., "Master-slave interferometry for parallel spectral domain interferometry sensing and versatile 3D optical coherence tomography," Opt. Express 21, 19324-19338 (2013).
[2] Rivet, S., Maria, M., Bradu, A., Feuchter, T., Leick, L., and Podoleanu, A., Complex master slave interferometry, Opt. Express 24, 2885-2904 (2016).
[3] Bradu A., and Podoleanu, A.,"Imaging the eye fundus with real-time *en-face* spectral domain optical coherence tomography," Biomed. Opt. Express. 5, 1233-1249 (2014).
[4] Bradu, A., Kapinchev, K., Barnes, F., and Podoleanu, A., "On the possibility of producing true real-time retinal cross-sectional images using a graphics processing unit enhanced master-slave optical coherence tomography system," J. Biomed. Opt., 20(7), 076008 (2015).
[5] Bradu, A., Rivet, S., and Podoleanu, A., "Master/slave interferometry – ideal tool for coherence revival swept source optical coherence tomography," Biomed. Opt. Express 7, 2453-2468 (2016).
[6] John, D., Burgner, C. B., Potsaid, B., Robertson, M. E., Lee, B. K., Choi, W, Cable, A. E., Fujimoto, J. Jayaraman, V., "Wideband electrically-pumped 1050 nm MEMS-tunable VCSEL for ophthalmic imaging," J. Lightwave Technol, **33**, 3461–3468, (2015).